SUPPORTING INFORMATION

Ligands make the difference! Molecular insights into Cr^{VI}/SiO_2 Phillips catalyst during ethylene polymerization.

Caterina Barzan,[a]* Alessandro Piovano,[a] Luca Braglia,[ab] Giorgia A. Martino,[a] Carlo Lamberti,[ab] Silvia Bordiga[a] and Elena Groppo[a]*

[a] Department of Chemistry and NIS Centre, University of Torino, via G. Quarello 15A, I-10135 Torino, Italy

[b] IRC "Smart Materials", Southern Federal University, Zorge Street 5, 344090 Rostov-on-Don, Russia

S1. Oxidation state and coordination geometry of the Cr sites active in ethylene polymerization: DR UV-Vis-NIR spectroscopy

The DR UV-Vis-NIR spectrum of the Cr^{VI}/SiO_2 catalyst reduced in ethylene prior polymerization is compared with those of Cr^{II} and Cr^{III} references in Figure S1a.

- The spectrum of the CO-reduced Cr^{II}/SiO_2 catalyst (dark blue) is dominated by two well defined d-d bands at 7500 and 12000 cm^{-1} assigned to Cr^{II} ions having a +2 oxidation state and a 4-folded coordination.[1-5] These bands blue shift when the Cr^{II} ions expand their ligand field up to a distorted octahedral coordination. For example, in the presence of CO the d-d bands shift up to 20000 cm^{-1}.[1, 3]

- The spectrum of $CrCl_3*6(H_2O)$ physisorbed on Aerosil SiO_2 (bold green) is that typical of 6-fold coordinated Cr^{III} ions, i.e. it shows two equally intense bands in the 15000–17000 cm^{-1} and 20000–25000 cm^{-1} regions attributed to the $^4A_2 \rightarrow {}^4T_2$ and $^4A_2 \rightarrow {}^4T_1$ transitions, respectively.[5-8]

- The spectrum of the Cr^{VI}/SiO_2 catalyst reduced in ethylene (red) is characterized by two d-d bands at 9500 cm^{-1} and 16700 cm^{-1} (having a shoulder at 15100 cm^{-1}) and three charge-transfer bands at 21500 cm^{-1}, 29500 and 40000 cm^{-1}. The assignment of this spectrum is not straightforward, also due to the fact that the catalyst is not yet completely reduced. Nevertheless, the d-d band at 9500 cm^{-1} is assigned to the first d-d transition of a Cr^{II} species, being too low in energy to be attributed to Cr^{III} ions. The band at 16700 cm^{-1} is assigned to the second d-d transition of Cr^{II} species in a distorted 6-fold geometry. Indeed, Cr^{II} ions in a perfect octahedral geometry, as for $Cr(H_2O)_6^{2+}$, show a single $^5E_g \rightarrow {}^5T_{2g}$ transition around ~14000 cm^{-1}.[9] A vertical distortion of the octahedral geometry results in the splitting of the transition in four separate contributions.[9] However, this is true in solution, in which the distortion is completely symmetrical; in the solid state and in a system governed by amorphous silica, the distortions of the octahedral metal sites cannot be ad symmetrical, thus might result in a lower number of transitions, characterized by heterogeneity and thus resulting in a broadening of the bands. Finally, we coupled the two d-d bands at 9500 and 16700 cm^{-1} also because they display a similar behavior as a function of the reaction time.

The ambiguity in the full assignment of the UV-Vis bands is due to the overlap of the low-energy charge-transfer region (i.e. O=Cr LMCT) and the high-energy d-d region (Cr^{III} $^4A_2 \rightarrow {}^4T_1$). This is the reason why the UV-Vis data require the XANES data counterpart in order to overcome possible wrong assignments (and VICEVERSA).

Figure S1b compares the spectrum of Cr^{VI}/SiO_2 catalyst reduced in ethylene at 150 °C (bold red) with that of the same catalyst reduced in cyclohexene at room temperature (light blue).[11] Cyclohexene is considered a model molecule that can simulate what is happening during the reduction of chromate species in the presence of an olefin (induction period), but without taking part to the subsequent polymerization reaction. Reduction of Cr^{VI} species in cyclohexene leads to 6-fold coordinated Cr^{II} sites in interaction with an ester molecule.[11] We wish to underline once more that this catalyst does not display Cr^{III} species, as verified by EPR spectroscopy (highly selective for Cr^{III} ions) The corresponding UV-Vis spectrum is characterized by two d-d bands at 10000 and 16500 cm^{-1}, very similar to those observed for Cr^{VI}/SiO_2 catalyst reduced in ethylene. Interestingly, the spectrum of Cr^{VI}/SiO_2 catalyst reduced in cyclohexene (light blue) does not show the shoulder at 15100 cm^{-1}, which might be attributed to a d-d transition of another reduced Cr species.
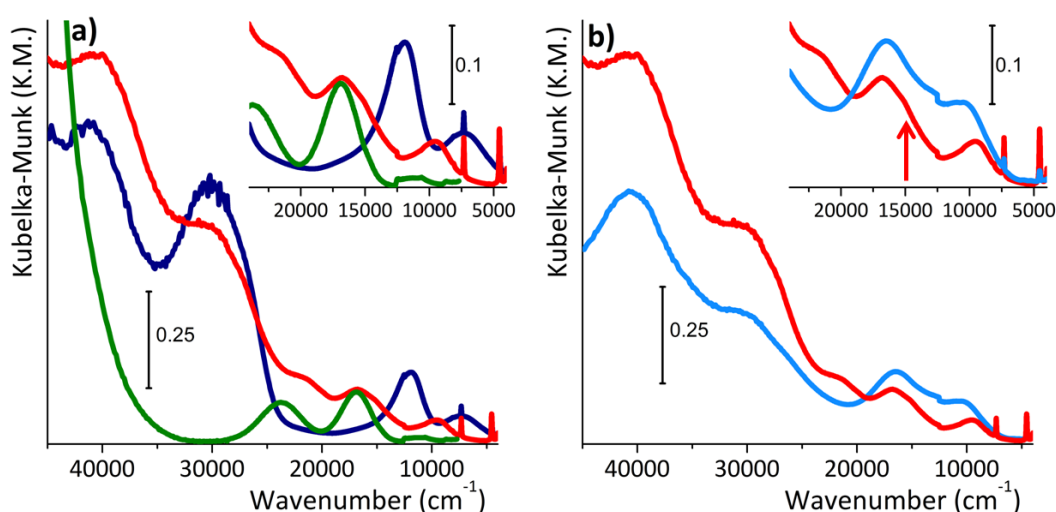

Figure S1: Part (a): DR UV-Vis-NIR spectra of Cr^{VI}/SiO_2 catalyst upon reduction in ethylene at 150 °C (bold red), upon reduction in CO at 350 °C (blue) and of the $CrCl_3*6(H_2O)$ complex physisorbed on Aerosil SiO_2 (green). Part (b): DR UV-Vis-NIR spectra of Cr^{VI}/SiO_2 catalyst reduced in ethylene at 150 °C (bold red), and after reduction in cyclohexene at room temperature (light blue). In both cases the insets show the magnification of the d-d spectral region.

S2. XANES spectroscopy: simulations

At first, we simulated the XANES spectra of a few DFT-optimized clusters representing Cr^{VI}/SiO_2, Cr^{II}/SiO_2 and Cr_2O_3 in order to validate our theoretical method. Calculations were performed by adopting a cluster approach[10] and Gaussian 09 software.[11] To model Cr^{VI}/SiO_2 and Cr^{II}/SiO_2 (in their highly dehydroxylated form), we adopted clusters having a brutto formula of $H_{10}O_{48+2}Si_{21}Cr$ (see the graphical representation in Figure S2 A and B). The chromium sites can be grafted on the silica surface in various positions. However, it was found that their geometry does not significantly influence the position of the main XANES features. For Cr_2O_3, the geometry of a small cluster (12 Å large) cut from the periodic structure of Cr_2O_3 and terminated with H atoms, was optimized at the same level of theory. In all the cases the computational cost was reduced by employing the ONIOM embedding approach[12] as already shown in our previous work.[4]

High-level calculations were performed by adopting the ωB97xD long-range corrected hybrid functional.[13] H atoms were described through a standard Pople-type 6-311++G(2d,2p) basis set;[14] Cr by an Ahlrichs TZVp (triple zeta valence plus polarization) basis set;[14] Si atoms through LanL2DZ pseudo-potential and the associated basis-set;[15] TZV2p Ahlrichs basis set was adopted to describe O atoms.[14] Low level is defined by employing the B97D functional;[16] H, Cr, and Si atoms are described with a 6-31G(d,p) basis set;[17] 6-31+G(d,p) basis set[18] was employed for O and C atoms. As dealing with open shell species [Cr(II)], the unrestricted formalism was adopted.

The XANES spectra of the Cr^{VI}/SiO_2, Cr^{II}/SiO_2 and Cr_2O_3 models discussed above were simulated using the sped up version of the FDMNES code[19,20] that uses the finite-difference method to solve the Schrödinger equation.[21] The cluster radius included in the calculation process was 5 Å from the Cr absorber. Hedin–Lundquist exchange and correlation potential were applied. XANES absorption spectra were modelled in the dipole and quadrupole approximation. Moreover, self-consistent calculations were performed, i.e. without imposing any restriction to the shape of the potential (i.e. beyond the *muffin-thin* approximation).[22] The theoretical spectra were convoluted by using an arctangent shape of the line broadening. Figure S2 compares the experimental and simulated XANES spectra for Cr^{VI}/SiO_2, Cr^{II}/SiO_2 and Cr_2O_3. The three experimental spectra are very well reproduced by our structural models, demonstrating the reliability of our method.

On the basis of the experimental results obtained with *operando* FT-IR and DR UV-Vis spectroscopies, the XANES spectrum of Cr^{II}/SiO_2 in interaction with methylformate and ethylene was also simulated. In the DFT-optimized cluster the methylformate ligand is arranged with the sp^2 oxygen of the O=C bond in interaction with the divalent Cr ion (see the graphical representation in Figure S3C). The simulated XANES spectrum (Figure S3, middle) perfectly matches the main features of the experimental one (Figure S3, left), confirming the results obtained with the other spectroscopic techniques.
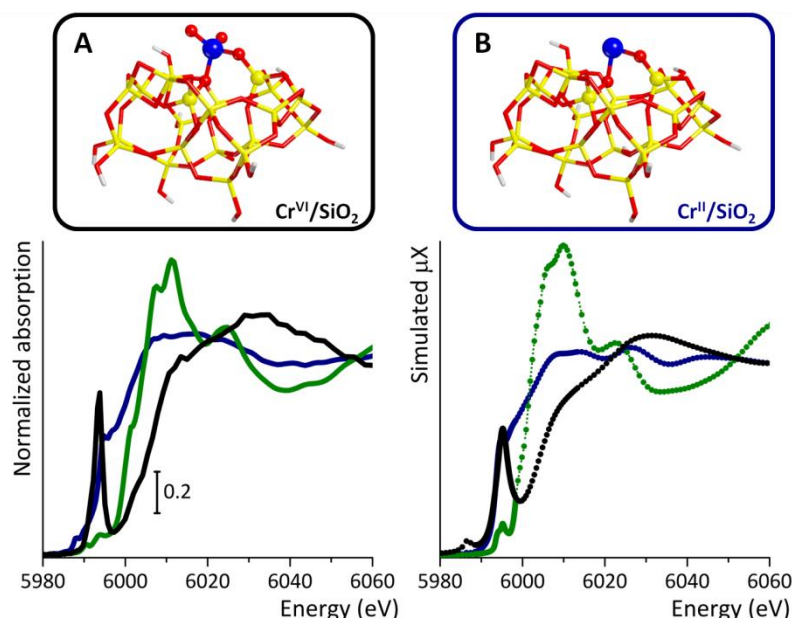

Figure S2: Top: Graphical representation of the clusters adopted to model Cr^{VI}/SiO_2 (A) and Cr^{II}/SiO_2 (B). The color code of the atoms is: white for H, yellow for Si, red for O, blue for Cr. Bottom: Experimental (left) and simulated (right) XANES spectra of Cr^{VI}/SiO_2 (black), Cr^{II}/SiO_2 (blue) and Cr_2O_3 (green).
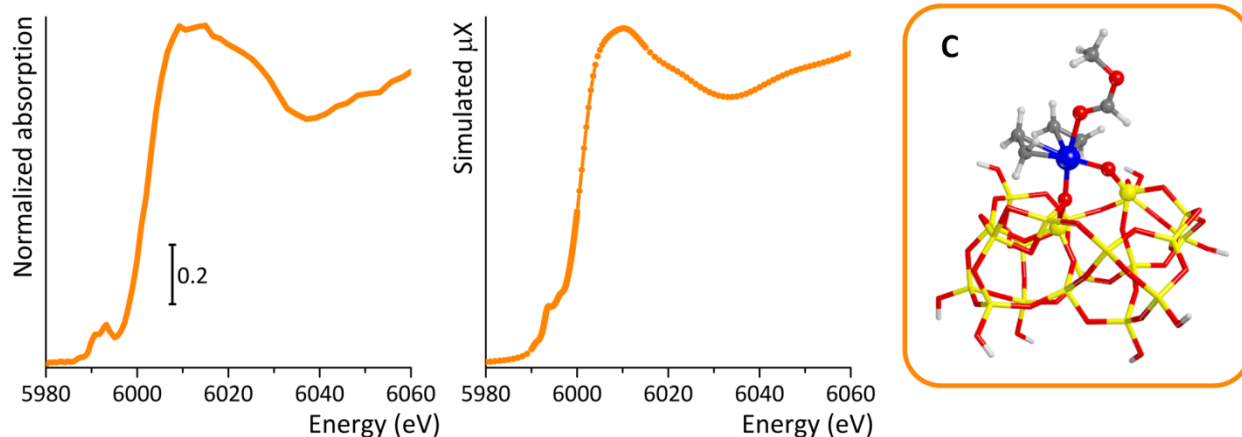
Figure S3: Experimental (left) and simulated (middle) XANES spectra of Cr^{VI}/SiO_2 reduced in ethylene. Right: Graphical representation of the clusters adopted to model Cr^{II}/SiO_2 in interaction with two molecules of ethylene and one of methylformate. The color code of the atoms is: white for H, yellow for Si, red for O, blue for Cr.

Last but not least, a remarkable achievement is given from the comparison of the calculated charge of the Cr ion in the mentioned models. The ionic charge is figured out with FDMNES code from the atomic number of the absorber less the number of electrons, which is calculated by integration of the density of electron up to the ionic radius (0.8 Å). In these cases, it is not important to consider the absolute value of ion charge but the relative value in the systems [23,24]: 3.2 in Cr^{VI}/SiO_2, 2.3 Cr_2O_3, 1.2 in Cr^{II}/SiO_2, and 0.9 in Cr^{II}/SiO_2 in interaction with methylformate. This result strengthens the hypothesis that we detect an intermediate Cr^{II} species in interaction with methylformate during the ethylene polymerization.

S3. Characterization of the ethylene oxidation by-products: FT-IR spectroscopy

Figure 3 in the main text (here proposed again for clarity as Figure S4) shows the FT-IR spectra of the Cr^{VI}/SiO_2 catalyst before (black) and after reduction in ethylene at 150 °C and removal of gaseous ethylene (red). The spectrum of Cr^{VI}/SiO_2 is that typical of an highly dehydroxilated silica, with in addition the two fingerprints of grafted chromates at 1980 cm^{-1} and 910 cm^{-1} (the latter in part e). When the catalyst is reduced in ethylene, new absorption bands appear in the 3050-2700 cm^{-1} region (part b, $v(CH_x)$), in the 1750-1500 cm^{-1} range (part d, $v(CO)$ due to the extremely high extinction coefficient, as already discussed in the main text) and in the 1500-1300 cm^{-1} region (part d, $\delta(CH_x)$). The partial reduction of the chromates is testified by the decrease of the two bands at 1980 cm^{-1} and 910 cm^{-1} (parts c –subtracted spectrum - and e, respectively).

The assignment of the IR absorption bands in the 3050-2700 and 1750-1300 cm^{-1} regions is not straightforward. Being two molecules of formaldehyde and a bare Cr^{II} site the most claimed product of ethylene oxidation on the Phillips catalyst during the induction time, efforts were devoted to understand whether these bands might be related to formaldehyde (HCHO) molecules adsorbed on Cr^{II} sites or on SiO_2. To this aim, formaldehyde was dosed at room temperature on a highly dehydroxlated SiO_2 (the same Aerosil used for the synthesis of Cr^{VI}/SiO_2) calcined at the same temperature that Cr^{VI}/SiO_2 (650 °C) and on Cr^{II}/SiO_2. The resulting spectra are shown in Figure S5. It must be noticed that pure formaldehyde is not available because it is highly

reactive. Thus we obtained it by the direct decomposition of paraformaldehyde at temperatures higher than 200 °C in vacuum.[25-28] Being also H_2O a side product of paraformaldehyde decomposition, the gas phase was passed through a trap containing anhydrous Na_2SO_4.

Parts A1 and A2 – Formaldehyde adsorbed on dehydroxylated silica

When formaldehyde is dosed on pure SiO_2 (light grey spectrum in Figure S5, A1 and A2) a sharp IR band is observed at 1730 cm^{-1}, which is assigned to the $v(C=O)$ of formaldehyde in interaction with the silica surface. The FT-IR spectra gradually change as a function of time (from light to dark grey). The band at 1730 cm^{-1} decreases in intensity, concomitantly to the growth of a series of IR absorption bands, assigned to polyoxymethylene (Table S1). [26, 28]

Table S1: Position (in wavenumbers, cm^{-1}) and assignment of the absorption bands in the FT-IR spectra of formaldehyde adsorbed on pure silica dehydroxylated at 650 °C.

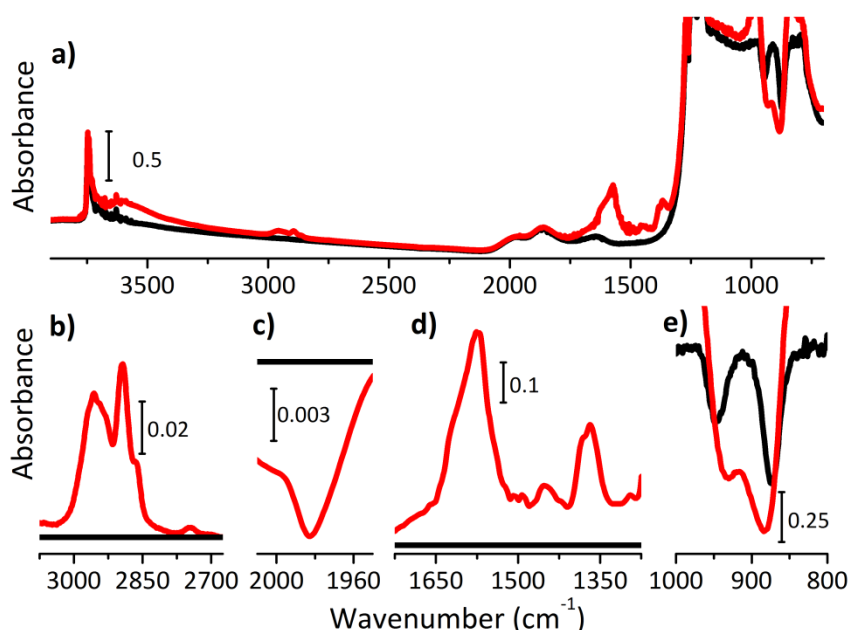| assignment	Polyoxymethylene on SiO_2	Formaldehyde on SiO_2
$v_{asymm}(CH_2)$	2980	
$v_{symm}(CH_2)$	2915	
$2w(CH_2)$	2797	
$v(CO)$		1730
$\delta(CH_2)$	1478	
$w(CH_2)$	1427	
$w(CH_2)$	1383	

Figure S4: FT-IR spectra of Cr^{VI}/SiO_2 before (black) and after reduction in ethylene at 150 °C (red). Part (a) shows the spectra in the whole 3800–700 cm^{-1} wavenumber region; parts (b) and (d) show magnifications in the spectral regions where the absorption bands characteristic of ethylene oxidation products give a contribution (spectra subtracted from that of Cr^{VI}/SiO_2); part (c) shows the magnification of the region in which the first overtone of the Cr=O mode of the chromate species contributes (subtracted spectra); part (e) reports a magnification of the region where the vibrational modes of silica perturbed by the presence of the chromates are visible.
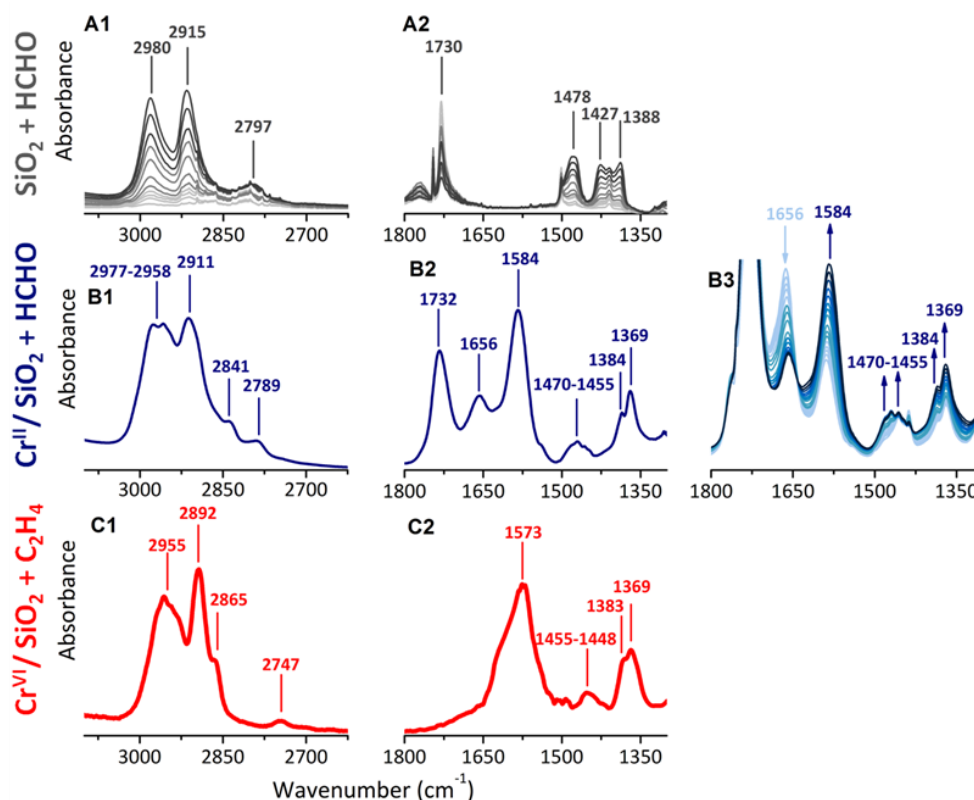
Figure S5: Parts A1 and A2: Time-resolved FT-IR spectra of highly dehydroxylated silica in interaction/reaction with an excess of formaldehyde. Parts B1-B3: FT-IR spectra of Cr^{II}/SiO_2 after reaction with formaldehyde and removal of the excess from the IR cell. The whole sequence of spectra collected during reaction of formaldehyde with Cr^{II}/SiO_2 are shown in part B3 (from light blue to blue). Parts C1 and C2: FT-IR spectra of Cr^{VI}/SiO_2 after reduction in ethylene. Column 1 shows the 3100-2600 cm^{-1} range where $v(CH_x)$ bands are expected, while column 2 shows the 1800-1500 cm^{-1} range, where the bands due to $v(C=O)$, $\delta(CH)$ modes give a contribution.

Table S2: : Position (in wavenumbers, cm^{-1}) and assignment of the absorption bands in the FT-IR spectra of formaldehyde adsorbed on the CO-reduced Cr^{II}/SiO_2 catalyst and of its products of reaction.

assignment	polyoxymethylene	formaldehyde on SiO_2	formaldehyde on Cr^{II}	methylformate on Cr^{II}
$v_{asymm}(CH_2)$	2977			
$v_{asymm}(OCO) + \delta(CH)$				2958
$v_{asymm}(CH_3)$				
$v_{symm}(CH_2)$	2911			
$v_{symm}(CH_3)$				2893 (shoulder)
$v(CH)$				2865 (shoulder)
$v_{symm}(CH_2)$		2841	2841	
$2w(CH_2)$	2789			
$v_{symm}(OCO) + \delta(CH)$				2745
$v(CO)$		1732		
$v(CO)$			1656	
$v_{asymm}(OCO)$				1584
$\delta(CH_2)$	1470			
$\delta(CH_3)$				1455
$\delta(CH_2)$			1455	
$\delta(CH)$				1384
$v_{symm}(OCO)$				1369

When formaldehyde is dosed on Cr^{II}/SiO$_2$, the FT-IR spectra evolve as a function of time (Figure S5 part B3 from light blue to blue) until an equilibrium is reached. The complexity of the spectra is due to the concomitance of the polymerization of formaldehyde on silica and of the reaction/interaction of formaldehyde with the Cr^{II} sites. The IR bands at 1732 and 1656 cm^{-1} have been assigned to the ν(C=O) of formaldehyde in interaction with SiO$_2$ and Cr^{II} sites, respectively. The growth of the IR bands at 1584, 1470, 1455, 1384 and 1369 cm^{-1} and the simultaneous decrease of that at 1656 cm^{-1} testifies that HCHO on the Cr^{II} sites is not stable, but it undergoes a molecular disproportionation leading to products more similar to formate or carboxylate species in which the ν(C=O) vibration is lower than 1600 cm^{-1} due to a weak C=O and C-O resonance. When formaldehyde is removed from the cell the IR band at 1732 cm^{-1} decreases in intensity testifying that the excess of HCHO is partially removed from the silica surface. The multitude of IR bands remaining upon outgassing has been assigned in Table S2 (based on the literature).[26, 29, 30] Moreover, based on our previous work involving the reaction of aldehydes with Cr^{II} species,[31] we have assigned the IR bands at 2958, 2745, 1584, 1455, 1384 and 1369 cm^{-1} to

methylformate generated from the Tishchenko reaction occurring between two molecules of formaldehyde on the Cr^{II} Lewis acid site.

Parts C1 and C2 – Cr^{VI}/SiO$_2$ catalyst reduced by ethylene at 150 °C

The spectrum of the ethylene reduced Cr^{VI}/SiO$_2$ catalyst is characterized by IR bands not easily attributable to formaldehyde in interaction with the catalyst surface or with reduced Cr sites. The vibrational manifestations are similar to those of formates or carboxylates, being the intense IR bands in the ν(CO) region lower than 1600 cm^{-1} (as discussed before). Based on the above assignment, we came to the conclusion that the main product of ethylene oxidation are two molecules of formaldehyde which are immediately converted to one methylformate molecule remaining in interaction with the just reduced Cr^{II} site. The extreme simplicity of the IR spectrum upon ethylene reduction leaves few doubts on the possibility that other products of oxidation, rather than methylformate, remain adsorbed on the catalyst surface. The assignment of all the IR bands is shown in Table 1 in the main text and is proposed again here in Table S3, along with a schematic representation of the reaction occurring during the induction period is shown in Scheme S1.
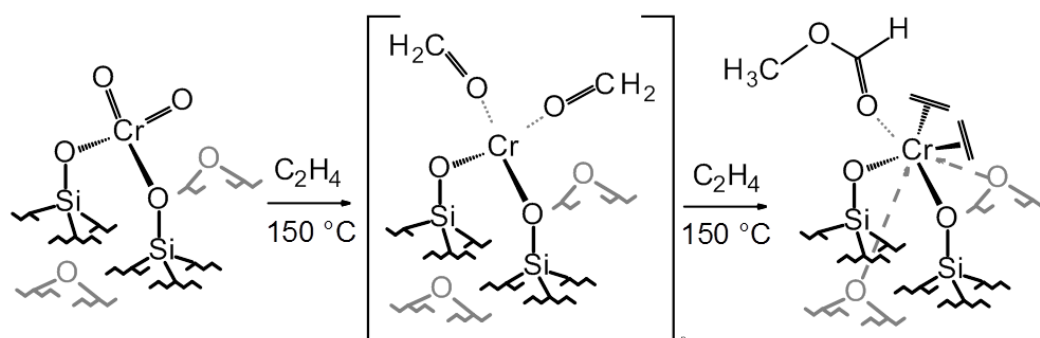
Scheme S1: Possible reaction pathway occurring between Cr^{VI}/SiO$_2$ Phillips catalyst and ethylene at 423 K during the induction period. The reduced Cr site is in interaction with methylformate and results in a Cr^{II} ion 6-fold coordinated.

Table S3: Position (in wavenumbers, cm^{-1}) and relative intensity (vs = very strong, s = strong, m = medium, w = weak) of the IR absorption bands attributed to ethylene oxidation products in interaction with the ethylene reduced Cr^{VI}/SiO$_2$ catalyst

Assignment	Methylformate on Cr^{II}
ν_{asymm}(OCO) + δ(CH) ν_{asymm}(CH$_3$)	2955 (s)
ν_{symm}(CH$_3$)	2892 (s)
ν(CH)	2865 (s)
ν_{symm}(OCO) + δ(CH)	2747 (w)
ν_{asymm}(OCO)	1617, 1573 (vs)
δ(CH$_3$)	1455 (m)
δ(CH)	1383 (s)
ν_{symm}(OCO)	1369 (vs)

S4. Application of Multivariate Curve Resolution – Alterning Least Squares (MCR-ALS) on the XANES spectra

Multivariate Curve Resolution - Alterning Least Squares (MCR-ALS) is a powerful chemometric algorithm that permits to decompose an experimental set of spectra into pure contributions, allowing to deriving the concentration profiles and the corresponding pure spectra of different species contributing to the experimental signals. Herein we applied the MCR-ALS algorithms in MATLAB, as described in Joaquim Jaumot *et al.*[32] Practically, it is recommended to introduce a set of constraints in order to suppress the ambiguity related to the algorithm solutions.[33] In this case, we imposed that the concentrations and the spectra of the pure components must be positive. Starting from this statement we run the PCA on the series of XANES spectra shown in Figure 1a in the main text. The analysis gave three main components, which their plot reconstruction with MCR-ALS is shown in Figure S6.

i) **Component 1**: the spectrum is the same as that of Cr^{VI}/SiO_2. We assign this component to monochromates.

ii) **Component 2**: the spectrum is similar to that collected at the end of the reaction (i.e. that of Cr^{VI}/SiO_2 after ethylene polymerization) and to the simulated XANES spectrum of cluster C in Figure S4. Consequently, this component is assigned to Cr^{II} in interaction with methylformate, which is the species active in ethylene polymerization.

iii) **Component 3**: this components is similar to Component 2 in terms of edge position and white line contribution, while it differs in terms of pre-edge features. This spectrum is assigned to the Cr species defined from the UV-Vis measurements as the spectator ones.
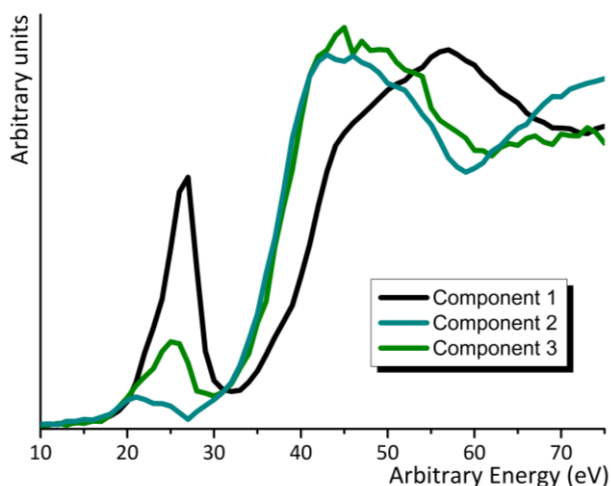

Figure S6: Principal Components resulting from the MCR-ALS

Figure S7 shows the evolution of the three Components during time (same color code). The same results are shown in the main text in Figure 2 (dashed curves). Component 1, assigned to the Cr^{VI} monochromate species, is the only present at the beginning and slowly decreases in concentration during the reaction. Component 2, assigned to the reduced active sites, keeps on growing in concentration, while Component 3, assigned to the reduced Cr sites acting as spectators, reaches a plateaux.
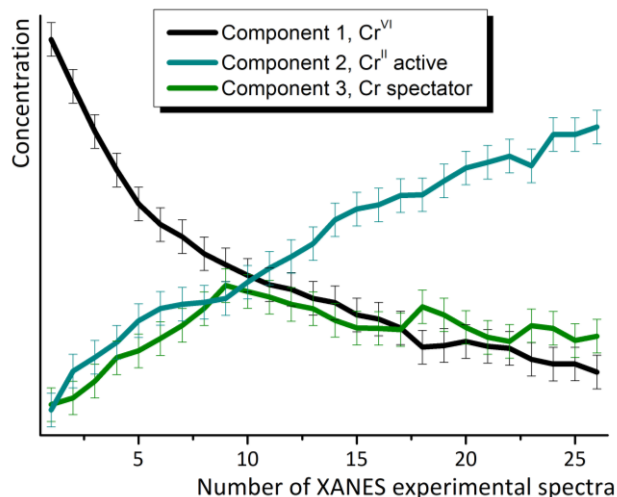

Figure S7: Evolution of Principal Component concentrations during time (the x-axis shows the number of spectra, each one collected in 12 minutes). The error bar is also introduced.

References

[1] E. Groppo, C. Lamberti, S. Bordiga, G. Spoto, A. Zecchina, *Chem. Rev.* **2005**, *105*, 115.

[2] E. Groppo, K. Seenivasan, C. Barzan, *Catal. Sci. Technol.* **2013**, *3*, 858.

[3] A. Budnyk, A. Damin, C. Barzan, E. Groppo, C. Lamberti, S. Bordiga, A. Zecchina, *J. Catal.* **2013**, *308*, 319.

[4] A. Budnyk, A. Damin, E. Groppo, A. Zecchina, S. Bordiga, *J. Catal.* **2015**, *324*, 79.

[5] B. M. Weckhuysen, L. M. Deridder, R. A. Schoonheydt, *J. Phys. Chem.* **1993**, *97*, 4756.

[6] B. M. Weckhuysen, I. E. Wachs, R. A. Schoonheydt, *Chem. Rev.* **1996**, *96*, 3327.

[7] A. Zecchina, E. Garrone, G. Ghiotti, C. Morterra, E. Borello, *J. Phys. Chem.* **1975**, *79*, 966.

[8] M. Cieslak-Golonka, *Coordin. Chem. Rev.* **1991**, *109*, 223.

[9] B. N. Figgis, *Introduction to ligand fields*, John Wiley & Sons, New York, **1966**.

[10] J. Sauer, P. Ugliengo, E. Garrone, V. R. Saunders, *Chem. Rev.* **1994**, *94*, 2095.

[11] M. J. Frisch, G. W. Trucks, H. B. Schlegel, G. E. Scuseria, M. A. Robb, J. R. Cheeseman, J. Montgomery, J. A., T. Vreven, K. N. Kudin, J. C. Burant, J. M. Millam, S. S. Iyengar, J. Tomasi, V. Barone, B. Mennucci, M. Cossi, G. Scalmani, N. Rega, G. A. Petersson, H. Nakatsuji, M. Hada, M. Ehara, K. Toyota, R. Fukuda, J. Hasegawa, M. Ishida, T. Nakajima, Y. Honda, O. Kitao, H. Nakai, M. Klene, X. Li, J. E. Knox, H. P. Hratchian, J. B. Cross, V. Bakken, C. Adamo, J. Jaramillo, R. Gomperts, R. E. Stratmann, O. Yazyev, A. J. Austin, R. Cammi, C. Pomelli, J. W. Ochterski, P. Y. Ayala, K. Morokuma, G. A. Voth, P. Salvador, J. J. Dannenberg, V. G. Zakrzewski, S. Dapprich, A. D. Daniels, M. C. Strain, O. Farkas, D. K. Malick, A. D. Rabuck, K. Raghavachari, J. B. Foresman, J. V. Ortiz, Q. Cui, A. G. Baboul, S. Clifford, J. Cioslowski, B. B. Stefanov, G. Liu, A. Liashenko, P. Piskorz, I. Komaromi, R. L. Martin, D. J. Fox, T. Keith, M. A. Al-Laham, C. Y. Peng, A. Nanayakkara, M. Challacombe, P. M. W. Gill, B. Johnson, W. Chen, M. W. Wong, C. Gonzalez, J. A. Pople, Revision B.05 ed., Gaussian, Inc., Wallingford CT, **2004**.

[12] S. Dapprich, I. Komaromi, K. S. Byun, K. Morokuma, M. J. Frisch, *J. Mol. Struct.-THEOCHEM* **1999**, *461*, 1.

[13] J.-D. Chai, M. Head-Gordon, *Phys. Chem. Chem. Phys.* **2008**, *10*, 6615.

[14] P. C. Hariharan, J. A. Pople, *Theor. Chim. Acta* **1973**, *28*, 213.

[15] J. P. Hay, W. R. Wadt, *J. Chem. Phys.* **1985**, *82*, 270.

[16] S. Grimme, *J. Comput. Chem.* **2006**, *27*, 1787.

[17] R. Ditchfield, W. J. Hehre, J. A. Pople, *J. Chem. Phys.* **1971**, *54*, 724.

[18] W. J. Hehre, R. Ditchfield, J. A. Pople, *J. Chem. Phys.* **1972**, *56*, 2257.

[19] S. A. Guda, A. A. Guda, M. A. Soldatov, K. A. Lomachenko, A. L. Bugaev, C. Lamberti, W. Gawelda, C. Bressler, G. Smolentsev, A. V. Soldatov, Y. Joly, *J. Chem. Theory Comput.* **2015**, *11*, 4512.

[20] A. A. Guda, S. A. Guda, M. A. Soldatov, K. A. Lomachenko, A. L. Bugaev, C. Lamberti, W. Gawelda, C. Bressler, G. Smolentsev, A. V. Soldatov, Y. Joly, *J. Phys.: Conf. Ser.* **2016**, *712*, Article N. 012004.

[21] Y. Joly, *Phys. Rev. B* **2001**, *63*, art. no. 125120.

[22] O. Bunau, Y. Joly, *J. Phys.-Condes. Matter* **2009**, *21*.

[23] G. Aullón, S. Alvarez, *Theor. Chem. Acc.*, **2009**, *123*, 67.

[24] F. Jensen, Introduction to Computational Chemistry, ISBN-13: 978-0-470-01186-7

[25] G. Busca, V. Lorenzelli, *J. Catal.* **1980**, *66*, 155.

[26] G. Busca, J. Lamotte, J. C. Lavalley, V. Lorenzelli, *J. Am. Chem. Soc.* **1987**, *109*, 5197.

[27] J. C. Lavalley, J. Lamotte, G. Busca, V. Lorenzelli, *J. Chem. Soc., Chem. Commun.* **1985**, 1006.

[28] F. Xamena, C. O. Arean, S. Spera, E. Merlo, A. Zecchina, *Catal. Lett.* **2004**, *95*, 51.

[29] J. F. Edwards, G. L. Schrader, *J. Phys. Chem.* **1985**, *89*, 782.

[30] V. Crocella, G. Cerrato, G. Magnacca, C. Morterra, F. Cavani, L. Maselli, S. Passeri, *Dalt. Trans.* **2010**, *39*, 8527.

[31] C. Barzan, A. A. Damin, A. Budnyk, A. Zecchina, S. Bordiga, E. Groppo, *J. Catal.* **2016**, *337*, 45.

[32] J. Jaumot, R. Gargallo, A. de Juan, R. Tauler, *Chemometr. Intell. Lab.* **2005**, *76*, 101.

[33] K. A. Lomachenko, E. Borfecchia, C. Negri, G. Berlier, C. Lamberti, P. Beato, H. Falsig, S. Bordiga, *J. Am. Chem. Soc.* **2016**, *138*, 12025.